STATE OF ALASKA

DEPARTMENT OF NATURAL RESOURCES

DIVISION OF GEOLOGICAL AND GEOPHYSICAL SURVEYS

Steve Cowper, *Governor*

Judith M. Brady, *Commissioner*

Robert B. Forbes, *Director and State Geologist*

August 1988

Report of Investigations 88-1

SEISMIC-HAZARD ANALYSIS OF THE NENANA AGRICULTURAL DEVELOPMENT AREA, CENTRAL ALASKA

by
Hans Pulpan

STATE OF ALASKA
Department of Natural Resources
DIVISION OF GEOLOGICAL & GEOPHYSICAL SURVEYS

According to Alaska Statute 41, the Alaska Division of Geological and Geophysical Surveys is charged with conducting 'geological and geophysical surveys to determine the potential of Alaskan land for production of metals, minerals, fuels, and geothermal resources; the locations and supplies of ground water and construction materials; the potential geologic hazards to buildings, roads, bridges, and other installations and structures; and shall conduct such other surveys and investigations as will advance knowledge of the geology of Alaska.'

In addition, the Division of Geological and Geophysical Surveys shall collect, record, evaluate, and distribute data on the quantity, quality, and location of underground, surface, and coastal water of the state; publish or have published data on the water of the state and require that the results and findings of surveys of water quality, quantity, and location be filed; require that water-well contractors file basic water and aquifer data, including but not limited to well location, estimated elevation, well-driller's logs, pumping tests, flow measurements, and water-quality determinations; accept and spend funds for the purposes of this section, AS 41.08.017 and 41.08.035, and enter into agreements with individuals, public or private agencies, communities, private industry, and state and federal agencies; collect, record, evaluate, archive, and distribute data on seismic events and engineering geology of the state; and identify and inform public officials and industry about potential seismic hazards that might affect development in the state.

Administrative functions are performed under the direction of the Director, who maintains his office in Fairbanks. The locations of DGGS offices are listed below:

.794 University Avenue
(Suite 200)
Fairbanks, Alaska 99709
(907)474-7147

.400 Willoughby Avenue
(3rd floor)
Juneau, Alaska 99801
(907)465-2533

.3700 Airport Way
Fairbanks, Alaska 99709
(907)451-2760

.18225 Fish Hatchery Road
P.O. Box 772116
Eagle River, Alaska 99577
(907)696-0070

This report is for sale by DGGS for $3.50. DGGS publications may be inspected at the following locations. Mail orders should be addressed to the Fairbanks office.

.3700 Airport Way
Fairbanks, Alaska 99709

.400 Willoughby Avenue
(3rd floor)
Juneau, Alaska 99801

.U.S. Geological Survey
Public Information Office
701 C Street
Anchorage, Alaska 99513

.Information Specialist
U.S. Geological Survey
4230 University Drive, Room 101
Anchorage, Alaska 99508

CONTENTS

	Page
Introduction	1
Earthquake source zones	3
Seismotectonic framework	3
Historic earthquakes	5
Seismic source-zone modeling	11
Seismicity	14
Maximum earthquake magnitudes	14
Seismicity rates	17
Attenuation relationships	19
Results and discussion	25
Conclusions	26
References cited	27

FIGURES

Figure	1.	Map showing location of study area	2
	2.	Map showing interaction area of the Pacific plate	3
	3.	Map showing seismicity and plate convergence along the Aleutian subduction zone and the Fairweather-Queen Charlotte fault system	4
	4.	Map section showing relationship between locations of historic earthquakes and large scale fault systems in interior Alaska	6
	5.	Map section showing areas of shallow seismicity (depths ≤ 40 km) in interior Alaska, 1982-85	8
	6.	Map section showing areas of shallow seismicity (depths < 20 km) in interior Alaska, 1968-85	9
	7.	Map layout of seismic-source zones in southcentral and interior Alaska	12
	8.	Map section showing areas of seismicity near NAG area based on all recorded data through June 1985	15
	9.	Graph of type-A attenuation relationships	20
	10.	Graph of type-B attenuation relationships	21
	11.	Graph of Woodward-Clyde attenuation relationships	22
	12.	Graph of Campell attenuation relationships	23
	13.	Graph showing comparison of attenuation relationships for M_s = 7.5 events	24

TABLES

Table	1.	Earthquakes ≥6.25 M_s in interior Alaska, 1904-68	10
	2.	Source-zone geographic coordinates	13
	3.	Source-zone seismicity rates	16
	4.	Parameters of the attenuation functions for peak acceleration	25

SEISMIC-HAZARD ANALYSIS OF THE NENANA AGRICULTURAL DEVELOPMENT AREA, CENTRAL ALASKA

by
Hans Pulpan[1]

INTRODUCTION

This report provides a seismic-hazard analysis of the Nenana Agricultural Development (NAG) area, located in central Alaska near the town of Nenana. The boundaries of the area are the Tanana River to the north and northeast, the Nenana River to the southeast, the Kantishna River to the west and the foothills of the Alaska Range to the south (fig. 1). For ease of calculation, the area is represented by a single site at 64.5° N. and 149.5° W, the center of the area.

The purpose of the analysis is to provide a quantitative basis for design in a seismically active area. Seismic design considerations are frequently based on the peak acceleration of ground motion (PGA) calculated for a particular period of interest and probability level of occurrence. The PGA value calculated herein has a 90-percent probability of not being exceeded in a 50-yr period. PGA, while not the only seismic-design parameter of consequence (particularly for critical facilities), does reflect well relative seismic hazard levels. This report also contains all non-site-specific information required to derive other ground-motion characteristics, for any desired period of interest and exceedence probability.

Three basic steps are needed to calculate seismic exposure values:

1) Identify seismotectonic structures, or seismic source zones capable of generating earthquakes, make geometric models of each, and determine earthquake recurrence rates and magnitude distribution for each.
2) Select relationships that describe the attenuation of desired exposure parameters as functions of distance to the site and earthquake magnitude.
3) Calculate the probability of occurrence of a given value of a ground-motion parameter on the basis both of attenuation relationship used, and probability of occurrence of earthquakes of different sizes at each seismic source zone. These calculations are made for a series of values, and the effect of all source zones is combined to derive a cumulative-distribution function of the exceedence probability for ground-motion parameters at the site.

These steps are common to most seismic-risk evaluations. Differences arise primarily in selecting the particular probability models used to describe earthquake occurrence and magnitude distribution and the sophistication with which the source zone geometry can be modelled. This probabilistic

[1]Geophysical Institute, University of Alaska-Fairbanks, Alaska 99775.

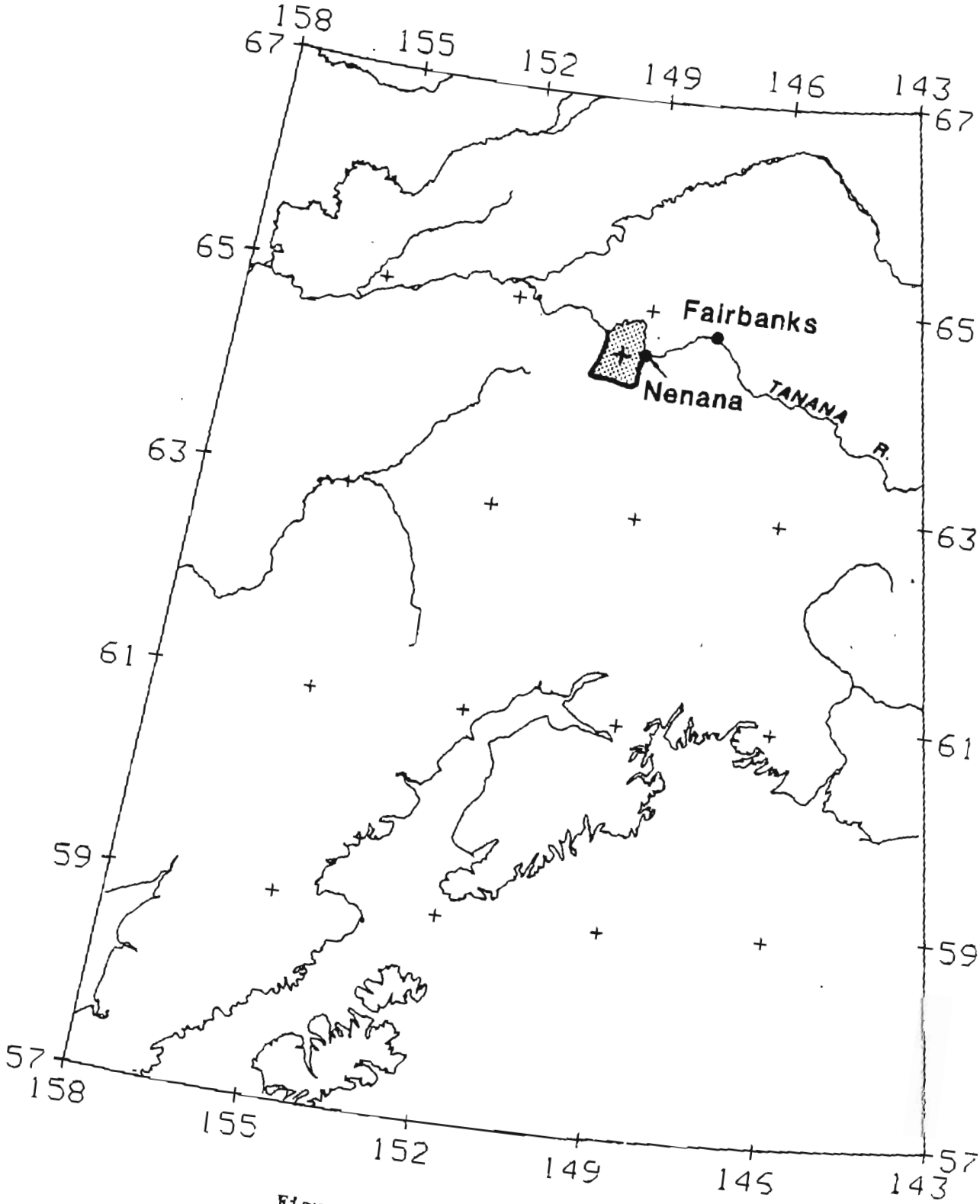

Figure 1. Study area location map.

approach helps mitigate our inability to predict the time of occurrence and size of earthquakes and our ignorance of the details of the physical processes which generate ground motion at a particular site. The particular approach chosen for this study is that of Mortgat and Shah (1979). The computer algorithm used to perform the calculations is based on the one developed by Woodward-Clyde Consultants (1982a).

EARTHQUAKE SOURCE ZONES

Seismotectonic Framework

The underlying cause of seismicity in Alaska is the relative motion between the Pacific and North American plates (figs. 2 and 3). Along the Fairweather-Queen Charlotte transform-fault system the two plates are slipping past one another in right-lateral motion. Along the Aleutian Island arc and the Alaska Peninsula, the Oceanic Pacific plate is underthrusting the continental North American plate. A fairly narrow belt of shallow, crustal seismicity along the Alaska panhandle traces the transform system. The wider belt of seismic activity along the arc reflects subduction of the oceanic plate. The subduction zone consists of an outer, shallow-dipping thrust zone between the subducted and subducting plates, and an arc-ward, more steeply

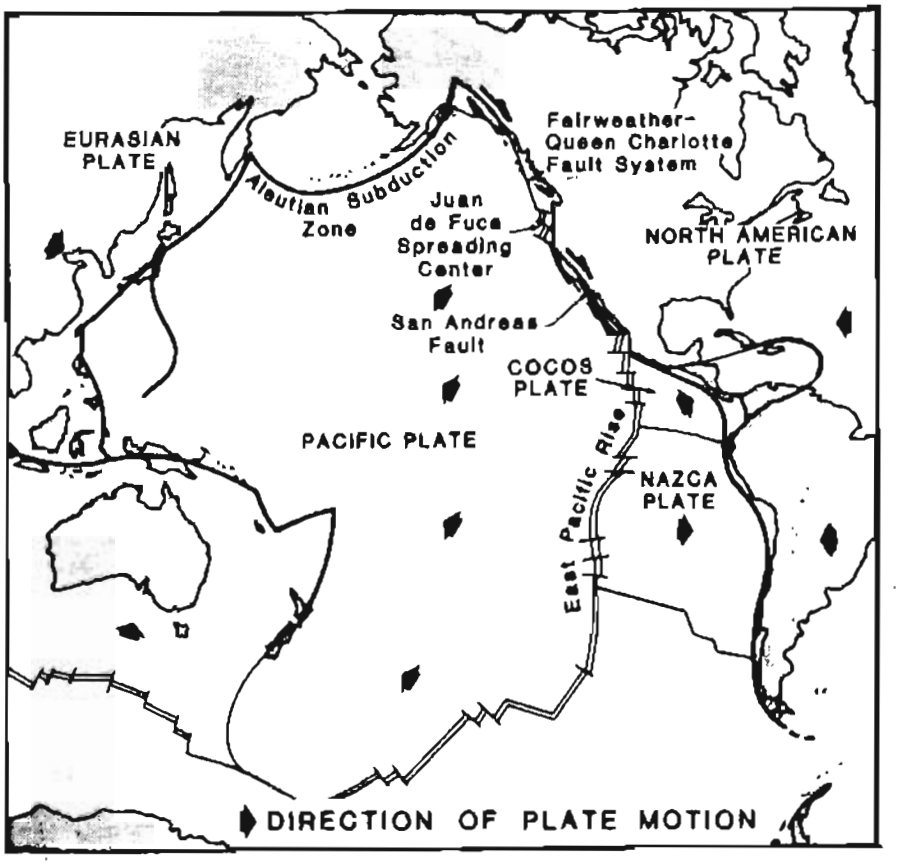

Figure 2. Interaction area of the Pacific plate (from Davis, 1984).

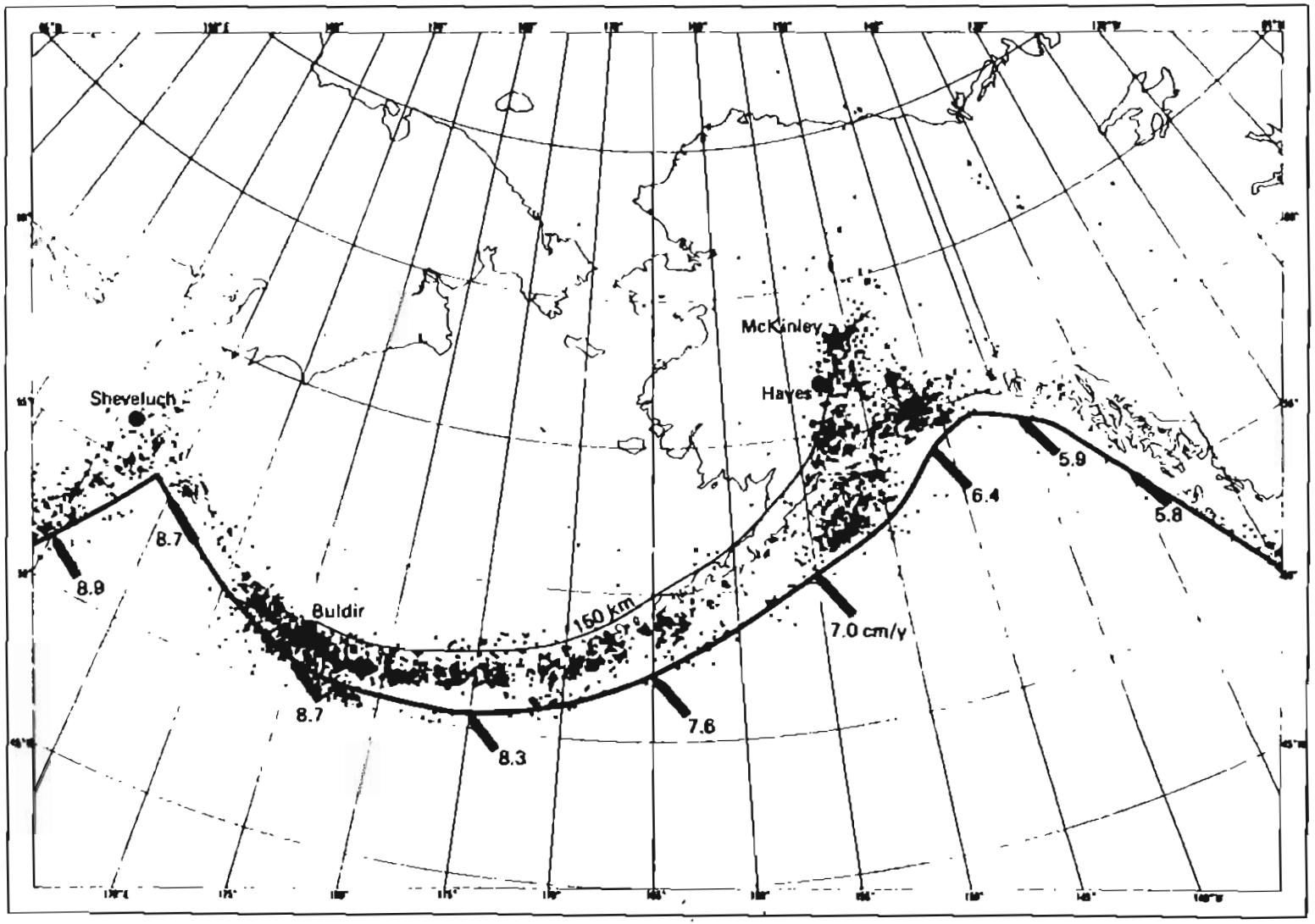

Figure 3. Areas of seismicity and plate convergence along the Aleutian subduction zone and the Fairweather-Queen Charlotte fault system. Solid curves indicate the trench and the 150-km depth contour of the Benioff zone (from Kienle and others, 1983).

dipping zone, termed the 'Wadati-Benioff zone.' This zone represents the brittle, seismically active interior part of the subducting plate. The widening of the seismic zone in southcentral Alaska reflects the widening of the thrust zone as the Wadati-Benioff zone and line of volcanoes start bending northward near lower Cook Inlet. The northernmost edge of the Wadati-Benioff zone is near 64° N., 40 km north of the Hines Creek strand of the Denali fault (Davies, 1975; Agnew, 1980).

Plate convergence generates stresses within the overriding plate also, resulting in a broad zone of intraplate seismicity, which decreases with distance from the plate boundaries. However, events of magnitude as large as M_s (maximum magnitude) = 7.3 have occurred as far as several hundred kilometers from these boundaries. Considering the location of the study site, intraplate seismicity constitutes the greater part of the seismic hazard.

Although the plate boundaries and Wadati-Benioff zones are fairly well delineated, it is not a straightforward matter to construct the intraplate source zones. Guidelines for constructing these zones might be obtained from the following section, which discusses the association between historic seismicity (especially larger events) and known or suspected fault systems.

Historic Earthquakes ($M_s \geq 6.25$)

Table 1 lists all earthquakes of magnitude $M_s \geq 6.25$ recorded between 63° and 67° N. latitude and 146° and 157° W. longitude. Several of the older events have been relocated both here and by other workers. In figure 4, these events are shown at what we consider their most accurate locations.

1. August 15, 1904 (M_s = 7.3) Although this was one of the largest events ever recorded in interior Alaska, it cannot be related directly to any known fault system. Wave-form analysis (Woodward-Clyde, 1982b) indicates that the event occurred in the crust and was associated with strike-slip motion. It may be associated with an unmapped continuation of the southern branch of the Tintina fault system, the Beaver Creek fault. Despite the relocation, the location of this event must be considered uncertain, given its early date.

2. July 7, 1912 (M_s = 7.2) This event is probably associated with the Hines Creek strand of the Denali fault system. Wave-form analysis (Woodward-Clyde, 1982b) indicates crustal (shallow) depth and a strike-slip mechanism.

3. January 21, 1929 (M_s = 6.5) This is one of several large events in the Tanana valley south of Fairbanks. It cannot be related to any mapped fault system. The event appears to be crustal in depth with a strike-slip mechanism (Woodward-Clyde, 1982b) and might be associated with a broad, east-southeast- to west-northwest-striking cluster of shallow seismicity that can be discerned from maps of recent (fig. 5) and historic (fig. 6) seismicity.

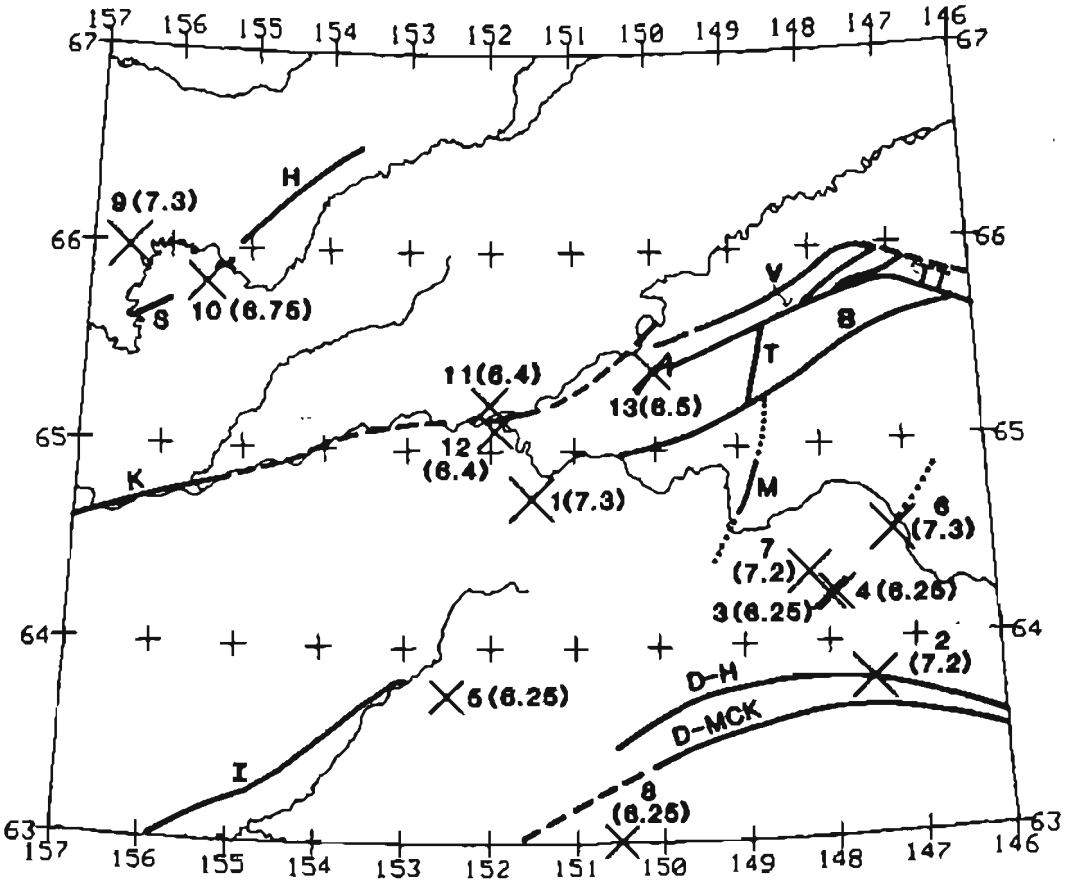

Figure 4. Relationship between locations of historic earthquakes ($M_s \geq 6.25$) and large scale fault systems in interior Alaska. Earthquake numbers correspond to those in table 1; numbers in brackets denote magnitudes. Solid curves are mapped faults (dashed where inferred). Dotted lines indicate seismically identified faults. B = Beaver Creek fault, D-H = Denali-Hines Creek strand, D-MCK = Denali-McKinley strand, H = Huslia fault, M = Minto fault, S = Shoestring fault, T = Tolovana fault, TT = Tintina fault, and V = Victoria Creek fault.

4. July 4, 1929 (M_s = 6.5) This event occurred within a few kilometers of the above one; thus, its relationship to any fault system is similarly enigmatic. It, too, appears to be a crustal event with strike-slip mechanism (Woodward-Clyde, 1982b).

5. September 4, 1935 (M_s = 6.25) This event conceivably could be associated with the Iditarod-Nixon fault, although it is located almost 50 km away. No known faults are closer to the epicenter, but no current evidence indicates the Iditarod-Nixon fault to be active.

6. July 22, 1937 (M_s = 7.3) This event, which occurred about 40 km southeast of Fairbanks, is not associated with any mapped fault. However, our relocation puts this event within a few kilometers of a seismic trend that is particularly sharp on the short-time seismicity map (fig. 5). A first-motion fault-plane solution of this event

(Adkins, 1940) indicates primarily strike-slip motion on either a N.30°E.- or N.43°W.-striking fault plane. Because the N.30°E.-striking plane is almost precisely that of the seismic trend, this event is most likely associated with a seismically defined fault zone that is presently active.

7. October 16, 1947 (M_s = 7.2) This is another large event in the Tanana valley south of Fairbanks, close to the two events of 1929. It cannot be related to any known faults, but could be associated with the seismic cluster noted above in the July 22, 1937 event.

8. August 19, 1948 (M_s = 6.25) The location and particularly the depth of this event indicate that it is associated with the Wadati-Benioff zones. The depth (90 km) appears to be well constrained by clear depth phases at several California seismic stations (Woodward-Clyde, 1982b).

9. April 7, 1958 (M_s = 7.3) The epicenter is about 40 km northwest of a series of southwest-northeast trending faults: the Huslia fault (Patton, 1966), the Shoestring Sand Dune fault (Weber and Péwé, 1970), and the Gusasa River fault (Bickel and Patton, 1957). Davis (1960) suggests a field epicenter on the Shoestring Sand Dune fault. A fault-plane solution (Ritsema, 1962) indicates normal faulting along a fault striking in the same direction as the mapped fault system and in the dominant direction of fracturing and collapse features observed by Davis (1960). This event may be associated with the Huslia fault system.

10. April 13, 1958 (M_s = 6.75) This aftershock of the April 7, 1958 earthquake is in line with both the Huslia and the Shoestring Sand Dune faults; as with the mainshock, it may be associated with the Huslia fault system.

11, 12. May 10, 1958 (M_s = 6.4) and May 11, 1958 (M_s = 6.4)

These events are very close to each other and very near to a mapped part of the Kaltag fault, with which they could be associated.

13. October 19, 1968 (M_s = 6.5) Known as the Rampart earthquake, this was the first event above magnitude 6 in central Alaska to be monitored by seismic instrumentation installed in several parts of Alaska in the wake of 1964's Good Friday earthquake. Thus, seismological information of considerable value is available for this event. First-motion fault-plane solutions of the mainshock and aftershock activity show that this event is associated with a shallow, steeply dipping strike-slip fault that trends north-south (Huang and Biswas, 1983). No previously mapped fault is associated with this aftershock zone, which crosses the Yukon river near today's Trans-Alaska Pipeline bridge; during construction a fault gouge was discovered there. This event typifies some of the problems in correlating historic earthquakes with tectonic features. Without the information derived from modern teleseismic and regional data, it would have been not unreasonable to associate this event with either the Tintina or the Victoria Creek faults. However, the seismic data show unequivocally that such an association is indirect at best and that no strain release on these faults was involved.

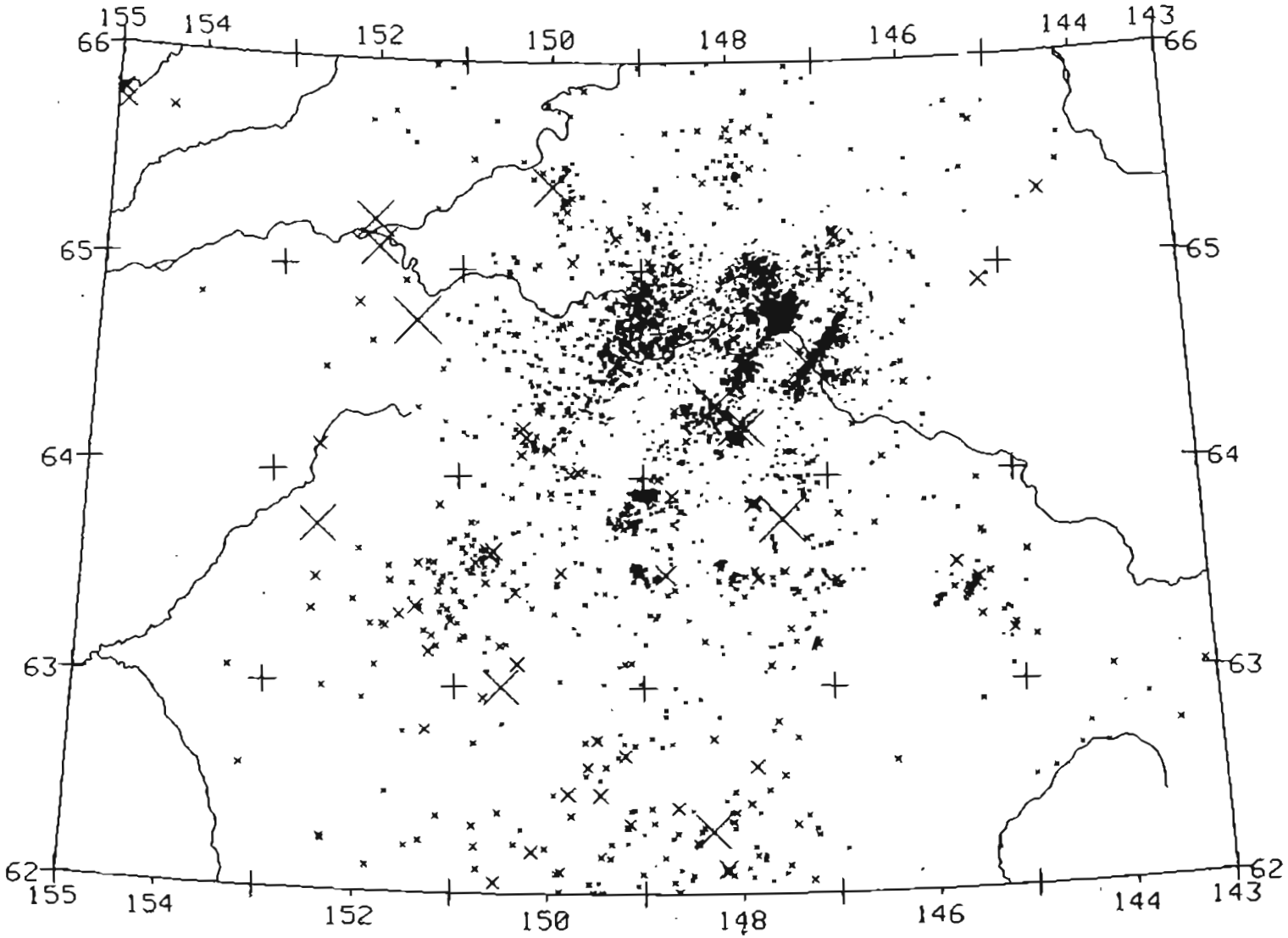

Figure 5. Areas of shallow seismicity (depths ≤ 40 km) in interior Alaska, 1982-85.

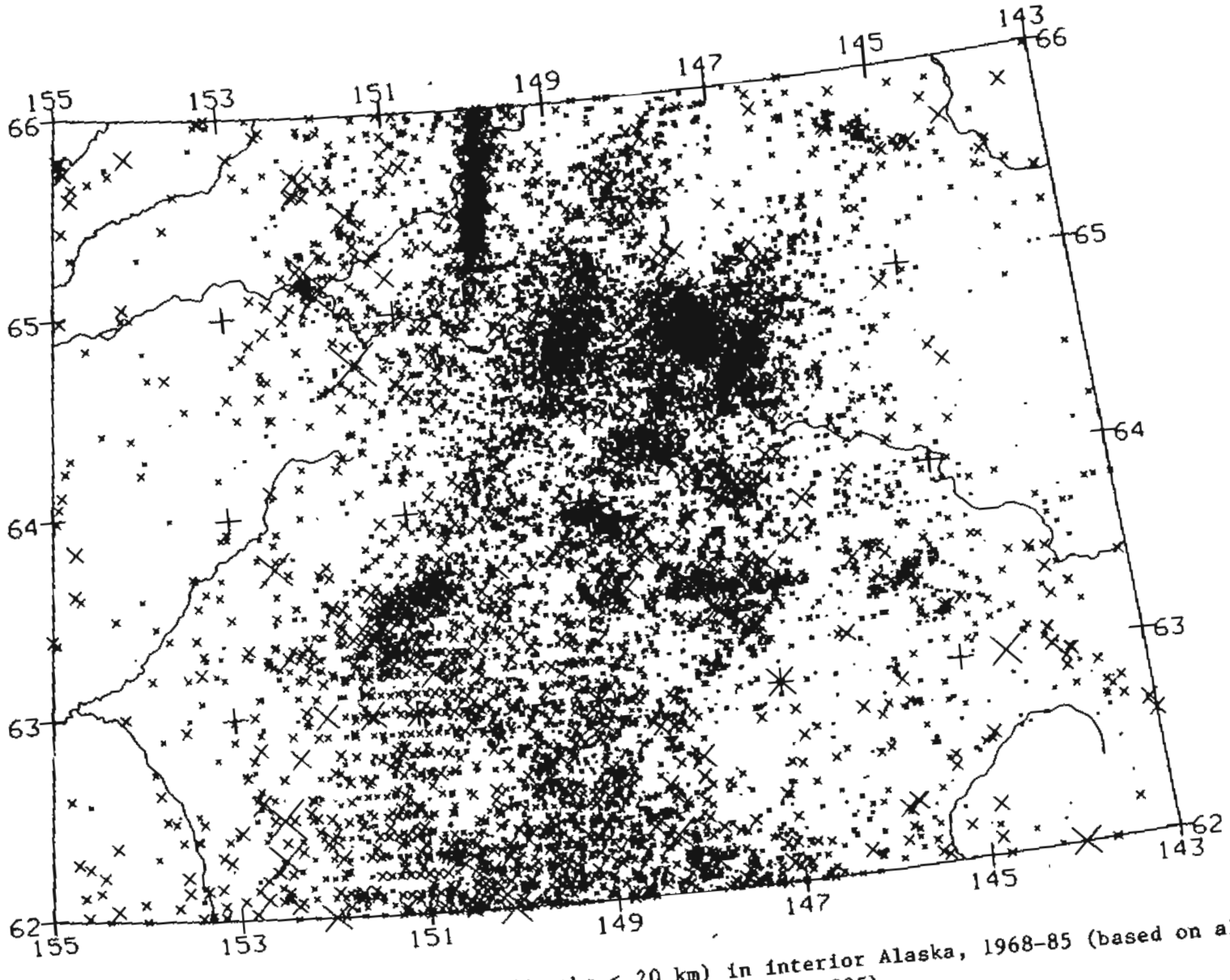

Figure 6. Areas of shallow seismicity (depths < 20 km) in interior Alaska, 1968-85 (based on all located earthquakes through June 1985).

Thus, considering the location uncertainties for pre-1960 events, many could have been associated with known faults such as the Denali, Iditarod-Nixon, Kaltag, and Huslia. Except for the Iditarod-Nixon fault, Holocene offsets have actually been documented on those faults. That such correlations can be erroneous has been discussed in connection with the 1968 Rampart earthquake. Other large historic earthquakes such as those in the Tanana valley, which is filled with Quaternary deposits, cannot be associated with mapped faults; however, one (no. 6, table 1) can be associated with a lineament of seismic activity that clearly delineates a seismically active fault. Such sharp delineation requires a fairly dense seismic network which, in the interior of Alaska, has been operated for an extended time only near Fairbanks. Hence, the concentration of seismic clusters in the Fairbanks area (fig. 5) might very well be an artifact of seismic-station distribution, and many such clusters might exist throughout the broad zone of seismic activity. Davies (1983) stated that the large historic events discussed here seem to define a southeast-northwest trending zone of seismic activity, which might be expected when a rigid indentor (the Pacific plate) impinges on a plastic medium (the North American plate); this is similar to the model proposed by Molnar and Tapponier (1975) for central Asia.

Table 1. Earthquakes ≥6.25 M_s in interior Alaska, 1904-68.

Event	Date	Latitude[a]	Longitude[a]	Magnitude[b]
1	08/27/04	64N(64.75N)[c]	151W(151.5W)[c]	7.3[d]
2	07/07/12	64N(63.8N)[e]	147W(147.5W)[e]	7.2[d]
3	01/21/29	64N(64.24N)[c]	148W(147.98)[c]	6.25
4	07/04/29	64N(64.24N)[c]	148W(147.88W)[c]	6.5
5	09/04/35	63.75N	152.5W	6.25
6	07/22/37	64.75N(64.55N)[f] (64.67N)[g]	146.75W(147.20W)[f] (147.58W)[g]	7.3[d]
7	10/16/47	64.5N (64.35N)[f] (64.2)[h]	148.60W(148.20W)[f] (149.0W)[h]	7.2[d]
8	08/19/48	63N	150.5W	6.25
9	04/07/58	66.03N(65.99N)[i]	156.59W(156.55W)[i]	7.3
10	04/13/58	66N(65.83N)[i]	156W(155.55W)[i]	6.75
11	05/10/58	65.23N	152.01W	6.4
12	05/11/57	65.10N	151.94W	6.4
13	10/29/68	65.4N(65.44)[j]	150.1W(150.00W)[j]	6.5

[a] Unless indicated otherwise, NOAA earthquake catalog locations are used.
[b] Unless indicated otherwise, NOAA earthquake catalog M_s is used.
[c] Relocated by Sykes (unpublished data).
[d] M_s redetermined by Abe and Noguchi (1983).
[e] Relocated by Woodward-Clyde Consultants (1982).
[f] Relocated during this study.
[g] Located by Adkins (1940).
[h] Located by St. Amand (1948).
[i] Relocated by Tobin and Sykes (1966).
[j] Located by Huang and Biswas (1983).

The NAG site and much of its surrounding area are overlain by Quaternary deposits, making fault detection difficult. Fault detection here is probably best achieved by monitoring seismic activity with a dense station network. A mosaic of fault-bounded tectonostratigraphic terranes, each having its own particular tectonic history, generates a situation where numerous planes of weakness exist; when combined with stresses transmitted by plate convergence, energy can be released in the form of earthquakes. Seismicity and tectonic style of the intraplate region in interior Alaska do not indicate a limited number of well-delineated seismic-source zones; rather, they suggest countless seismically active lineaments that have not yet been resolved throughout most of the region.

Seismic Source-Zone Modeling

Plate boundaries and Wadati-Benioff zones

These zones are well delineated by various regional seismic networks. The shallow thrust zone was modeled between the eastern margin of the 1964 Alaska earthquake rupture zone and the southern tip of the Kenai Peninsula. To accommodate the change in width and strike, two segments were used (fig. 7). Similarly, two segments were used to model the corresponding Wadati-Benioff zones. Table 2 lists geographic coordinates and depths of all the nodes which were used to construct the source zones. Note that the computer algorithm requires area sources to be constructed as trapezoids with the parallel sides at different depths.

Intraplate source zones

Except for two faults, all intraplate seismicity was modeled by two 'random-source' zones. 'Random' expresses the stipulation that earthquakes will occur with equal likelihood everywhere throughout the zone. The shape of the northern random zone reflects the trend indicated by the large historic events, and the southern random zone reflects the broad northerly trend of intraplate seismicity overlying part of the Wadati-Benioff zone. The southern zone extends farther to the south, but has been truncated here at a latitude beyond which the seismicity of this zone will not influence seismic exposure.

A 500-km-long section of the Denali fault, westward from where the Totschunda fault merges with it, has been modeled as a separate source zone within the southern random zone. The significance of the central section (nearest the NAG area) of the Denali fault for present-day seismotectonics is especially enigmatic. The 1912 (M_s = 7.2) earthquake appears to be the only large historic event associated with the fault; seismicity studies from regional networks (Tobin and Sykes, 1966; Page and Lahr, 1971) indicate that seismic activity is occurring in its vicinity. Geologic data from the central section (Hickman and Craddock, 1973) suggest various displacement rates during Holocene times, but there is no documentation of fault displacement during historic times. Hickman and others (1976) suggested that the latest movement occurred from several hundred to several thousand years ago. Nonetheless, statewide and regional seismic-hazard studies (Woodward-Clyde, 1982a-c; Thenhaus and others, 1985) include the Denali fault as a specific source zone, and it is modeled here as a vertical fault consisting of three

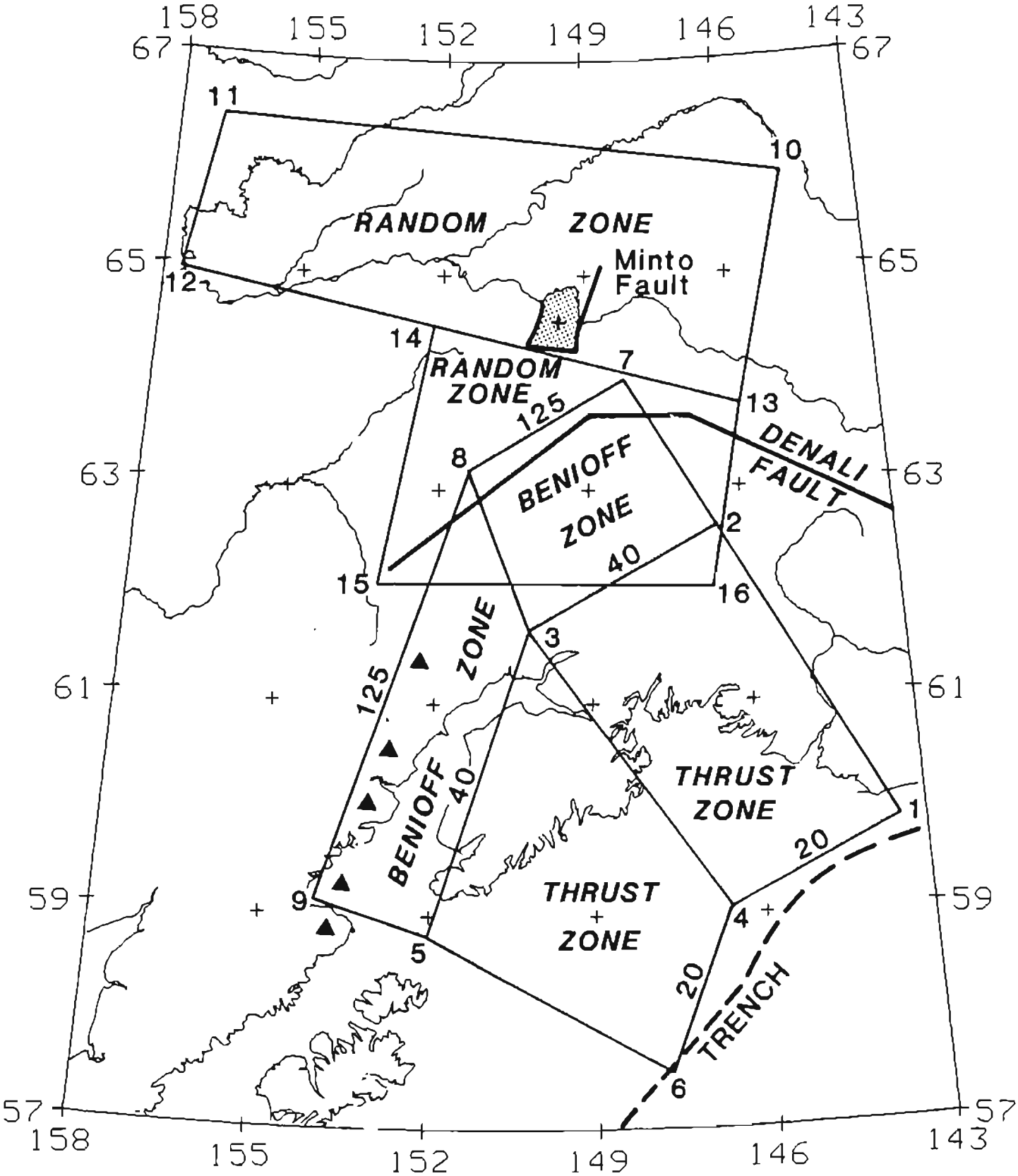

Figure 7. Map layout of seismic-source zones in southcentral and interior Alaska.

linear segments. Of the two strands in the central section, only the Hines Creek strand--the northern one--has been modeled.

The Minto fault was modeled as a separate source zone within the northern random zone because of its closeness to the NAG area. This fault trends northeast from the town of Nenana in Quaternary deposits but does not disrupt flood-plain alluvium or other deposits of recent age, and is expressed as a scarp as high as 4 m with the southeast side thrown up (Brogan and others, 1975). Barnes (1961) presented evidence from gravity surveys

Table 2. Source-zone geographic coordinates.

Node	Longitude (°W)	Latitude (°N)	Depth (km)
1	143.35	59.74	20
2	146352	62.62	40
3	150.07	61.63	40
4	146.41	58.90	20
5	152.08	58.81	40
6	147.78	57.22	20
7	148.22	64.09	125
8	151.25	63.22	125
9	154.00	59.09	125
10	145.00	66.00	10
11	157.00	66.80	11
12	157.00	65.00	11
13	146.00	63.80	11
14	152.00	64.55	10
15	152.50	62.00	10.5
16	146.70	62.00	10.5
17	144.00	63.00	10
18	146.90	63.60	10
19	149.00	63.60	10
20	153.00	62.40	10
21	148.60	65.20	10
22	149.20	64.50	10

Source zone	Nodes	Area (in km^2)
Shallow thrust east	1 2 3 4	73,000
Shallow thrust west	4 3 5 6	75,000
Benioff north	2 7 8 3	38,000
Benioff south	3 8 9 5	55,000
Random source north	10 11 12 13	114,000
Random source south	13 14 15 16	85,000
Denali fault	17 18 19 20	L = 520 km
Minto fault	21 22	L = 70 km

that the Minto fault represents a surface contact between Birch Creek schist and the flood-plain alluvium, with the northwest side being downthrown. The original mapping of Péwé and others (1966) indicates a fault length of 20 km.

The fault is modeled here based on seismic evidence, which indicates a south-southwest to north-northeast striking feature, the northern terminus at the Beaver Creek fault and the southern one just south of Nenana (fig. 8). The largest event of this seismic trend had a magnitude M_L (local magnitude) = 4.2. A composite fault-plane solution from 12 small events by Gedney (pers. commun.) indicates dip-slip faulting on a N.18°W.-trending fault. This trend is transverse to the trend indicated by the seismicity. The Minto fault may represent part of a complex horst-and-graben system; it is modeled here as a linear vertical fault, 70 km long, trending as indicated by the seismicity.

SEISMICITY

Maximum Earthquake Magnitudes

The magnitude of the largest earthquake to be taken into account for each source zone has to be decided for exposure calculations. These values are summarized, together with seismicity rates, in table 3.

Thrust zones

For shallow thrust zones, maximum magnitude was taken as 8.5. Although earthquakes as large as M_w (moment magnitude) = 9.2 have occurred on the Aleutian-Alaska thrust zone, this study chose a smaller value for several reasons. That section of the thrust zone modeled here ruptured in a great earthquake only about 20 yr ago, and the system is probably not sufficiently 'recharged' to generate an earthquake greater than M_s = 8.5 within the 50-yr time frame of the exposure calculation. Furthermore, peak ground acceleration values (aside from site topographic and geological effects) are influenced more by the dynamics of the stress release on high-strength patches of the rupture plane than by the total rupture area, which influences moment magnitude values. Empirical (Campell, 1981) and theoretical (Hadley and Helmberger, 1980) studies indicate both magnitude and distance saturation of peak ground-acceleration values.

To accommodate rupture areas associated with earthquakes in the M_w = 9.0 range, the modeled section of the shallow thrust zone would have to be extended, which appears unwarranted because of the reasons discussed above. Moreover, because of the great distances involved, such a zone extension would have little influence on exposure at the site.

Benioff zones

For the Wadati-Benioff zone, a maximum value of M_s = 7.5 was assumed. No earthquake larger than that has been recorded for that zone in the Aleutian-Alaska arc system, and only three events clearly associated with the Wadati-Benioff zone have been recorded elsewhere (Woodward-Clyde, 1982a).

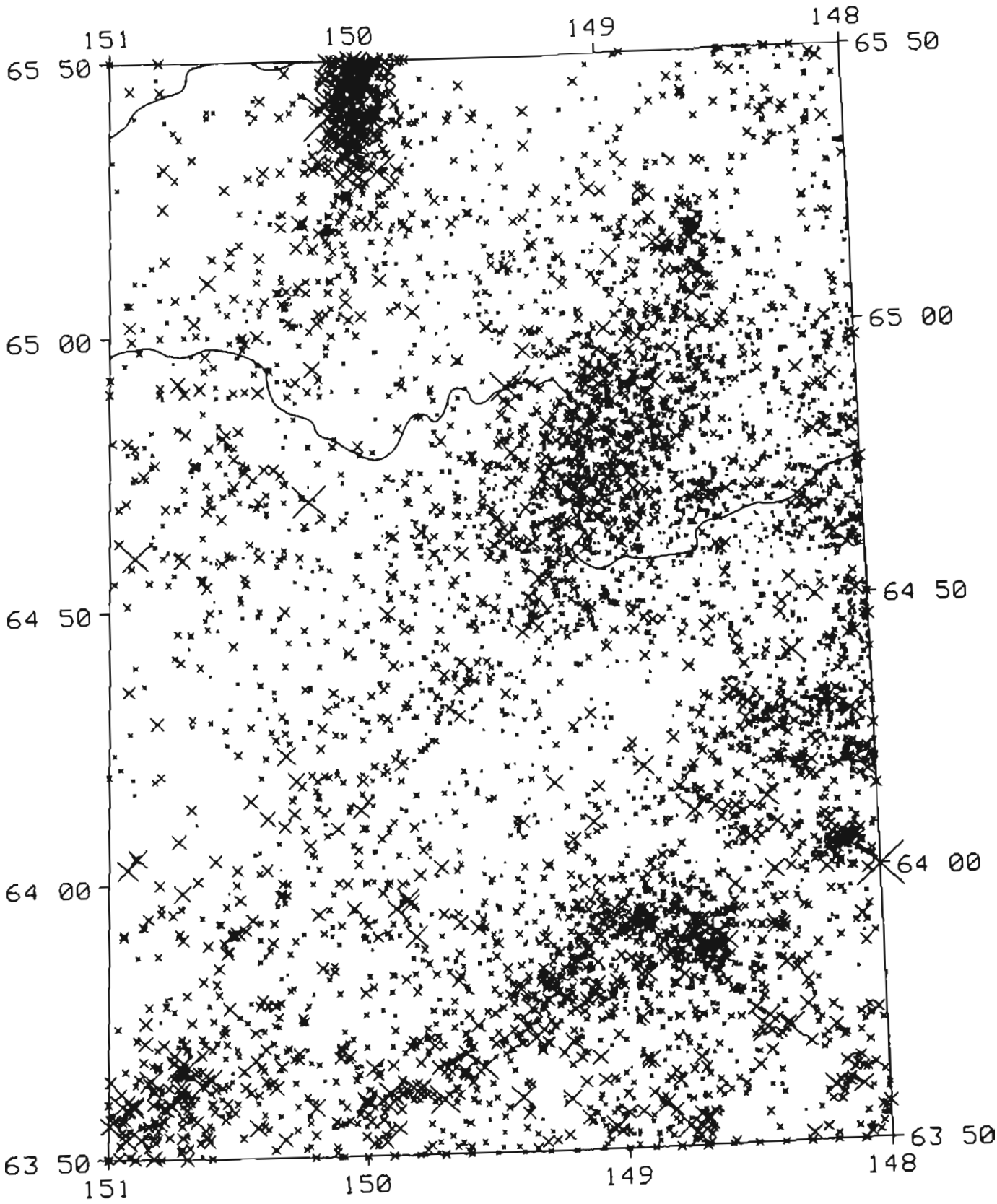

Figure 8. Areas of seismicity near NAG area based on all recorded data through June 1985.

Table 3. Source-zone seismicity rates.

Source zone	Study[a]	M_{max} (M_s)	b value	Events $M_s \geq 5$ (yr)[b]	Events $M_s \geq 7$ (yr)[b]	Return period M_{max} (yr)[b]
Shallow thrust	NAG	8.5	0.85	2.6×10^{-2}	5.9×10^{-4}	3.2×10^{4}
	OCS	8.5	0.80	1.4×10^{-2}	3.4×10^{-4}	6.7×10^{4}
	WWC1	8.5	0.85	3.1×10^{-2}	6.3×10^{-4}	3.0×10^{4}
	WWC2	9.5	0.70	2.0×10^{-2}	7.9×10^{-4}	7.0×10^{4}
	H-L	9.5	0.80	1.0×10^{-2}	2.5×10^{-4}	4.0×10^{5}
	Thenhaus	8.5	0.60	--	--	--
Wadati-Benioff	NAG	7.5	0.68	0.68×10^{-2}	2.9×10^{-2}	7.4×10^{3}
	OCS	7.5	0.55	0.95×10^{-2}	8.8×10^{-4}	--
	WWC1	7.5	0.68	0.68×10^{-2}	2.9×10^{-4}	7.4×10^{3}
	WWC2	7.5	0.90	3.9×10^{-2}	6.3×10^{-4}	4.4×10^{3}
	H-L	7.5	0.60	1.31×10^{-2}	12.6×10^{-4}	1.4×10^{3}
	Thenhaus	8.5	0.73	--	--	--
Random source south	NAG	7.5	0.80	0.9×10^{-2}	1.5×10^{-4}	9.2×10^{4}
	OCS	7.0	1.60	1.82×10^{-2}	0.44×10^{-4}	6.9×10^{4}
Random source north	NAG	7.5	0.8	1.2×10^{-2}	2.0×10^{-4}	8.4×10^{3}
	Thenhaus	7.3	0.8	--	--	--
Denali fault	NAG	8.0	0.85	9.0×10^{-2}	1.8×10^{-3}	3.9×10^{3}
	OCS	8.0	0.75	7.2×10^{-2}	2.2×10^{-3}	3.4×10^{3}
	WWC1	8.0	0.85	12.0×10^{2}	2.2×10^{-3}	3.1×10^{3}
	Thenhaus	8.5	0.60	--	--	--
Minto fault	NAG	7.0	1.0	7.6×10^{-2}	0.76×10^{-3}	1.3×10^{3}

[a] NAG = present study;
OCS = Woodward-Clyde Consultants, 1982a;
WWC1 = Woodward-Clyde Consultants, 1982b;
WWC2 = Woodward-Clyde Consultants, 1982c;
H-L = Harding-Lawson Associates, 1984;
Thenhaus = Thenhaus and others, 1985.

[b] These values are normalized to 1,000 km^2 for area sources and to 100 km for faults.

[c] These rates are for the Benioff zone between lower Cook Inlet and Anchorage, corresponding roughly to our southern Benioff zone.

-- = data not available for these categories.

Random sources

Maximum magnitude of the random source zone was set at 7.5, based primarily on the historical record, which shows three M_s = 7.3 events to be the largest events over the past 80 yr. The period for which one would expect earthquakes of this size to have been recorded or documented probably goes back about 90 yr.

There are a number of large-scale fault systems within this source zone that, based solely on their extent and continuity, could conceivably be associated with earthquakes larger than M_s = 7.5. But the role of these systems in present-day seismotectonics is unclear, though many of them have been shown to be seismically active (Estabrook, 1985). These large-scale features are probably expressions of a much earlier period in the evolution of Alaska when they were of more tectonic significance.

Denali fault

The maximum value for the Denali fault was taken to be M_s = 8.0. It is difficult to rationally assign a maximum value for this fault. Considering the fact that only one large historic earthquake (M_s = 7.2) can reasonably be associated with it, the large value assigned is principally based on the fact that it is such a dominant and extensive tectonic feature. Design criteria for the crossing of the Trans-Alaska Pipeline stipulated in almost a priori fashion a maximum value of M_s = 8.0. Woodward-Clyde (1982b) derived the same value, on the basis of: (a) a total fault length of 1,080 km; (b) the stipulation that only about 30 percent of the total length will rupture during a single earthquake; and (c) the relationship derived by Slemmons (1977) between rupture length and magnitude for strike-slip faults. However, determination of what constitutes a continuous fault length is not a straightforward matter.

Minto fault

The cluster of seismic activity that appears to be associated with the Minto fault extends about 70 km. Assuming that only 50 percent of the continuous fault segment will rupture in a single earthquake, and using Slemmons' (1977) empirical relationship between rupture length and magnitude for normal faults, one obtains a maximum magnitude of 7.0 for the Minto fault.

Seismicity Rates

Table 3 summarizes the seismicity rates used for the various source zones and information on the rates assumed by various other seismic hazards studies.

Thrust zones

The recurrence rates used are based primarily on rates derived from historical data by Jacob and Hauksson (1983) for the whole Aleutian-Alaskan arc, and adjusted here because this source zone models only about 400 km of

the arc. Also, because the Jacob and Hauksson rates include Wadati-Benioff zone seismicity, only 85 percent was taken to apply to the shallow thrust zone. The resulting recurrence rates are quite similar to those of WWC1 (table 3), which are based on a regionally derived b-value and are consistent with a return period of 160 yr for the 1964 Prince William Sound earthquake as estimated by Davies and others (1981).

Wadati-Benioff zones

For the northern zone, the rates of Woodward-Clyde (1982b) were used because they are based on detailed studies of an area that is part of this source zone. The rates of Woodward-Clyde (1982c), which are based on historic data from an area between the southern tip of Kodiak Island and just north of Anchorage, were also used for the southern zone. The considerably higher seismicity rate of this zone is probably due to the high rate of activity beneath Iliamna volcano. Because such a high-activity cluster exists also beneath Mt. McKinley, and straddles the boundary between the northern and southern zone, these high rates might also be applicable to the northern zone.

Random source zones

Seismicity rates for the northern zone are based on the following assumptions: a b value of 0.8; a seismic moment rate of $5{,}314 \times 10^{25}$ dyn-cm/yr (based on the historic record); and a maximum magnitude of 7.5. From these assumptions, the a value in the Gutenberg-Richter relationship can be established (Dong and others, 1984).

The b value is taken from Thenhaus and others (1985), who derived their value from historic seismicity data for a source zone that is quite similar to the present one, although it extends considerably farther west. Davis and others (1978) derived a b value of 0.814 from a 68-yr data set for the Fairbanks area, which lies in the eastern part of the source zone.

The seismic-moment rate is based on all $M_s \geq 6.25$ earthquakes in the zone over an 80-yr period. The relationship of Thatcher and Hanks (1973) was used to convert M_s into seismic moment.

Recurrence rates assigned to the southern random zone were 75 percent of those assigned to the northern zone, because the Denali fault, which runs through this zone, has been modeled separately. The two random zones represent similar tectonic regimes. Because the southern zone is closer to the plate boundary, one might expect higher rates there. However, the section modeled shows a lower rate of large events. The only crustal events of $M_s \geq 6$ are the 1912 ($M_s = 7.2$) event, which is probably associated with the Denali fault, and the $M_s = 6.25$ event of 1935 (fig. 4; table 1). An $M_s = 7.3$ event (Nov. 3, 1943) occurred at 63.9° N., 151.3° W. (Woodward-Clyde, 1982b) just south of the source zone. The apparent lower rates could be an artifact of the catalog because of its limited time coverage. Alternatively, the lower rates might indicate that considerable seismic (and, in part, aseismic) strain release occurs along the Denali fault or that the plate behaves more rigidly in this area.

Denali fault

Recurrence rates for the Denali fault are based on a seismic moment rate of 3.0×10^{25} dyn-cm/yr, a b value of 0.85, and a maximum magnitude of 8.0.

The moment rate is based on an average slip rate of 1 cm/yr over the 500-km part of the fault modeled. Various studies have been conducted to infer displacement rates on this fault. Data by Hickman and Craddock (1973) from the Nenana River area suggest a displacement rate of 1.3 cm/yr for Holocene times. Stout and others (1973) estimate displacement rates of 0.5 to 0.6 cm/yr in Holocene times for a part of the fault east of the Black Rapids Glacier. Other studies (Plafker and others, 1977; Hickman and others, 1976) find evidence supporting displacement on the fault in historic times (Woodward-Clyde, 1982a). In calculating the moment rate from the slip rate, this study also assumed a fault width of 20 km and a value of 3×10^{11} dyn/cm^2 for the rigidity modulus (μ) of the fault-zone material.

Minto fault

Recurrence rates for the Minto fault are based on a and b values determined from a 13-yr (1968-1981) period of the earthquake catalog.

ATTENUATION RELATIONSHIPS

There are not enough strong-ground-motion recordings from Alaska to produce attenuation relationships based entirely on Alaska data. Seismic-hazard studies in the state have therefore made use of a variety of relationships. Thenhaus and others (1985) used the Schnabel and Seed (1973) relationships, which are based on early western United States data. Woodward-Clyde (1982a-c) used relationships derived from worldwide (primarily Japan) subduction-zone data for a seismic-risk study of the Gulf of Alaska, and relationships based on Imperial Valley, California earthquakes for work in Anchorage (Woodward-Clyde, 1982c), and yet another set of relationships for a hazard study of the Susitna hydroelectric project (Woodward-Clyde, 1982b).

In the present study, two separate sets of attenuation relationships were used, depending on source zone type. For earthquakes associated with shallow thrust zones and the Wadati-Benioff zone, the type-B relationship of Woodward-Clyde (1982a) was used. Comparison with Alaska data from these zones indicates that the type-B relationships are conservative (Jacob and Mori, 1984). For the intraplate source in the overriding plate, the study used the type-A relationship of Woodward-Clyde (1982a). However, use of relationships based on western United States data can be justified, and two derived from California data (Woodward-Clyde, 1982c; and Campell, 1981) were used for comparison. Campell's (1981) relationships are included here because he was particularly concerned with near-source attenuation and used worldwide data recorded within 50 km of earthquake rupture zones. His data do, however, include subduction-zone earthquakes. The attenuation relationships are graphed individually in figures 9 through 12, and figure 13 provides a comparison of the relationships for an $M_s = 7.5$ earthquake. Table 4 lists the parameters for attenuation relationships used in this study.

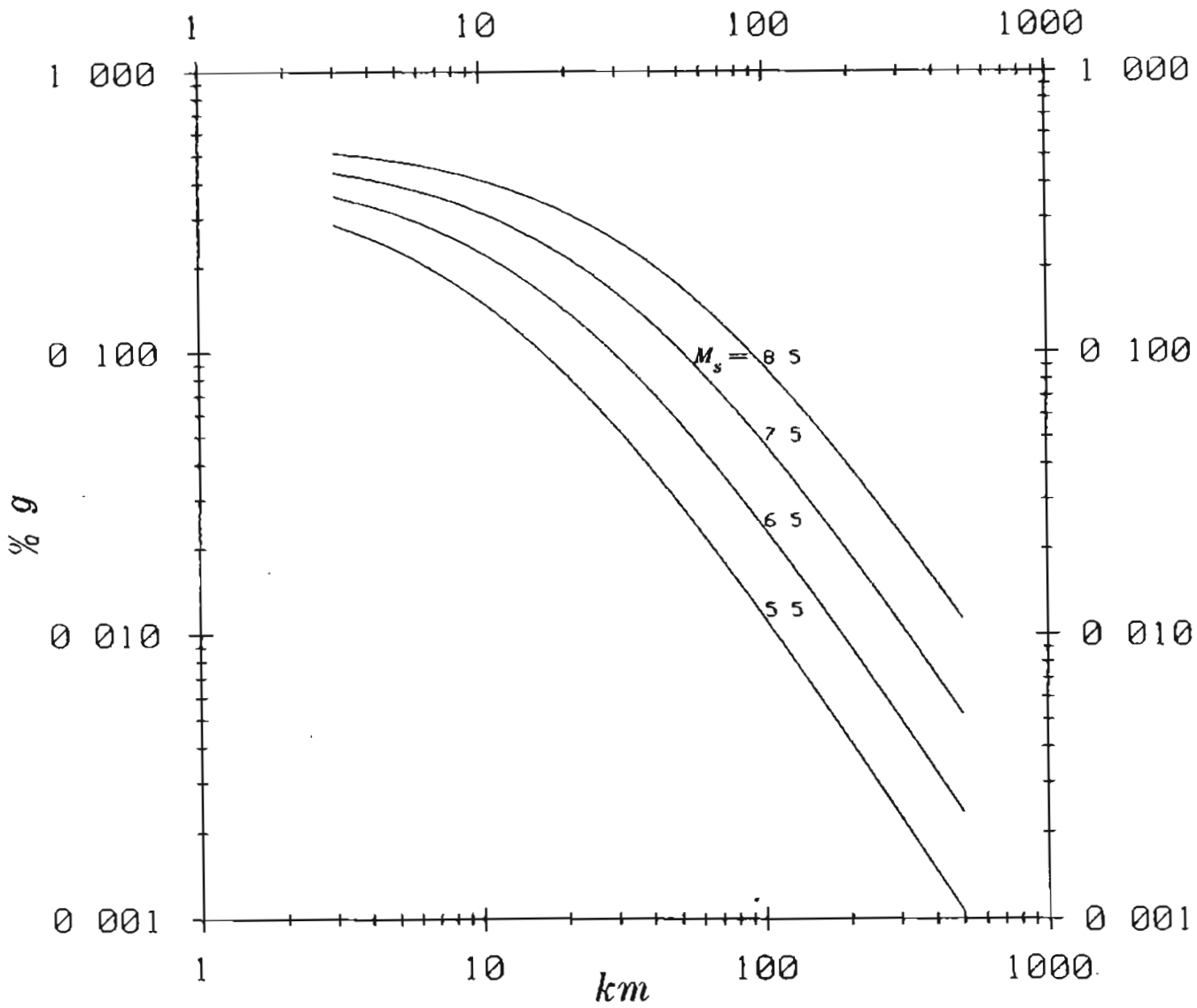

Figure 9. Type-A attenuation relationships. Peak ground acceleration (in % of g) as a function of surface wave magnitude (M_s) and distance (in km).

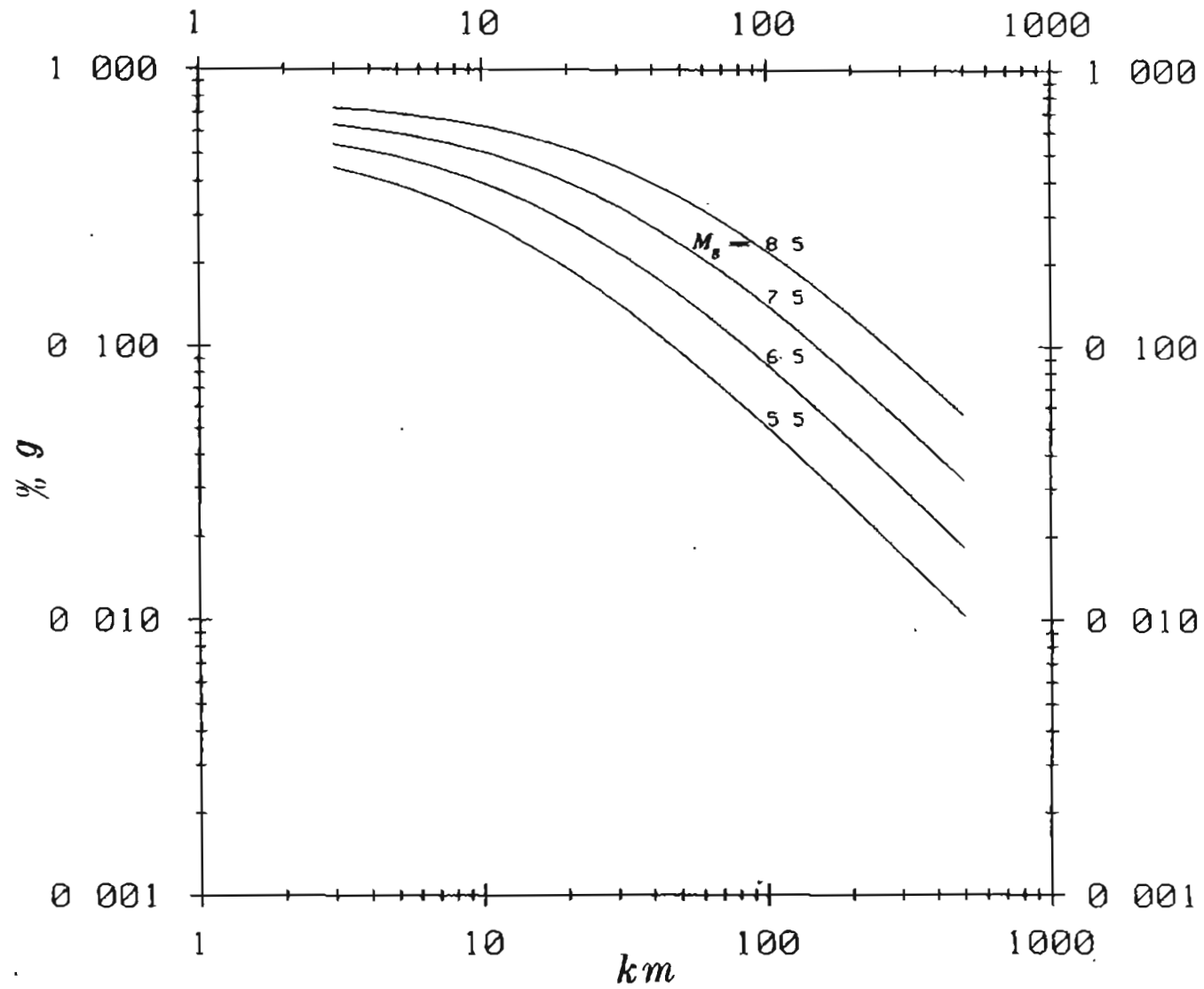

Figure 10. Type-B attenuation relationships. Peak ground acceleration (in % of g) as a function of surface wave magnitude (M_s) and distance (in km).

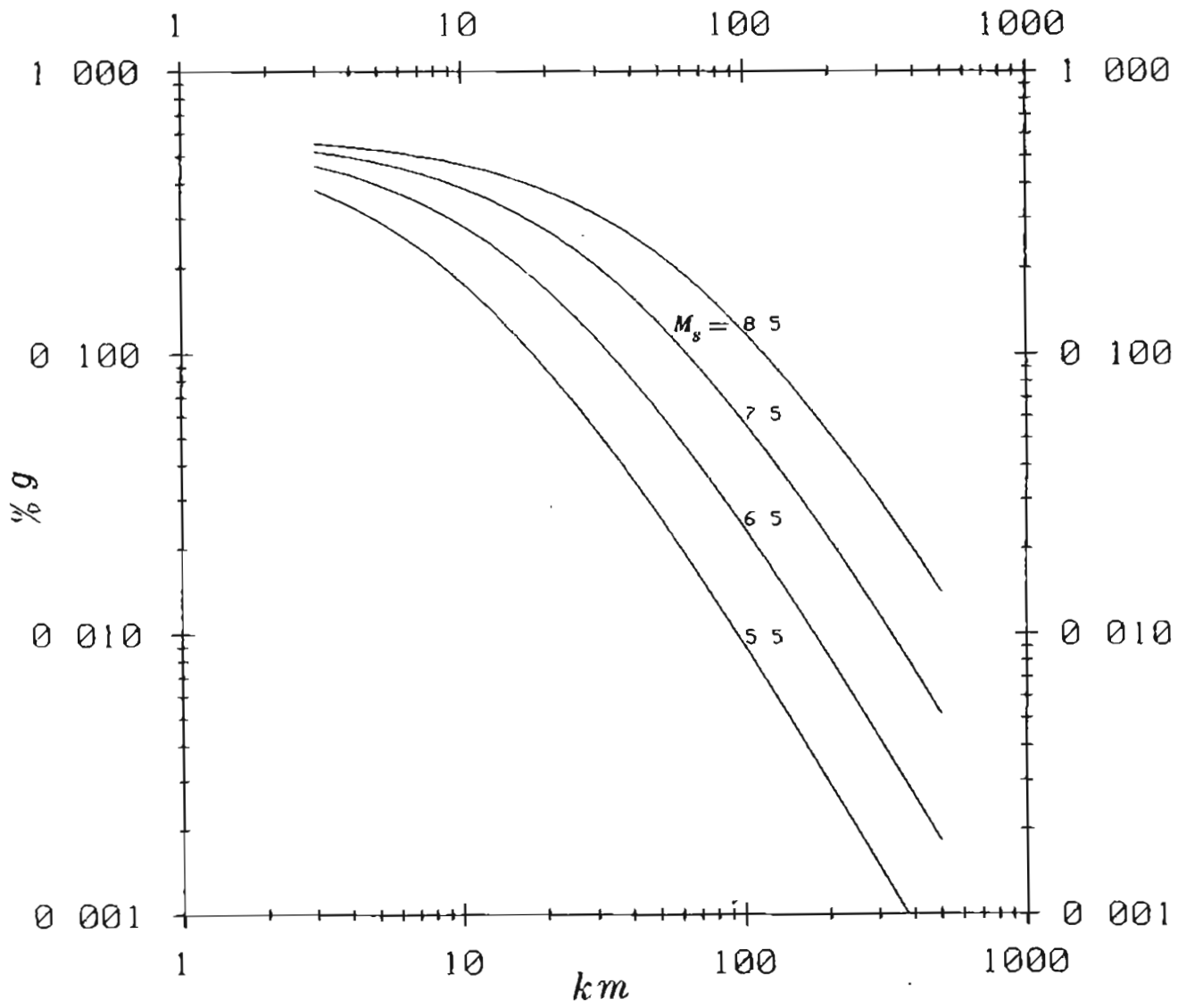

Figure 11. Woodward-Clyde (1982c) attenuation relationships. Peak ground acceleration (in % of g) as a function of surface wave magnitude (M_s) and distance (in km).

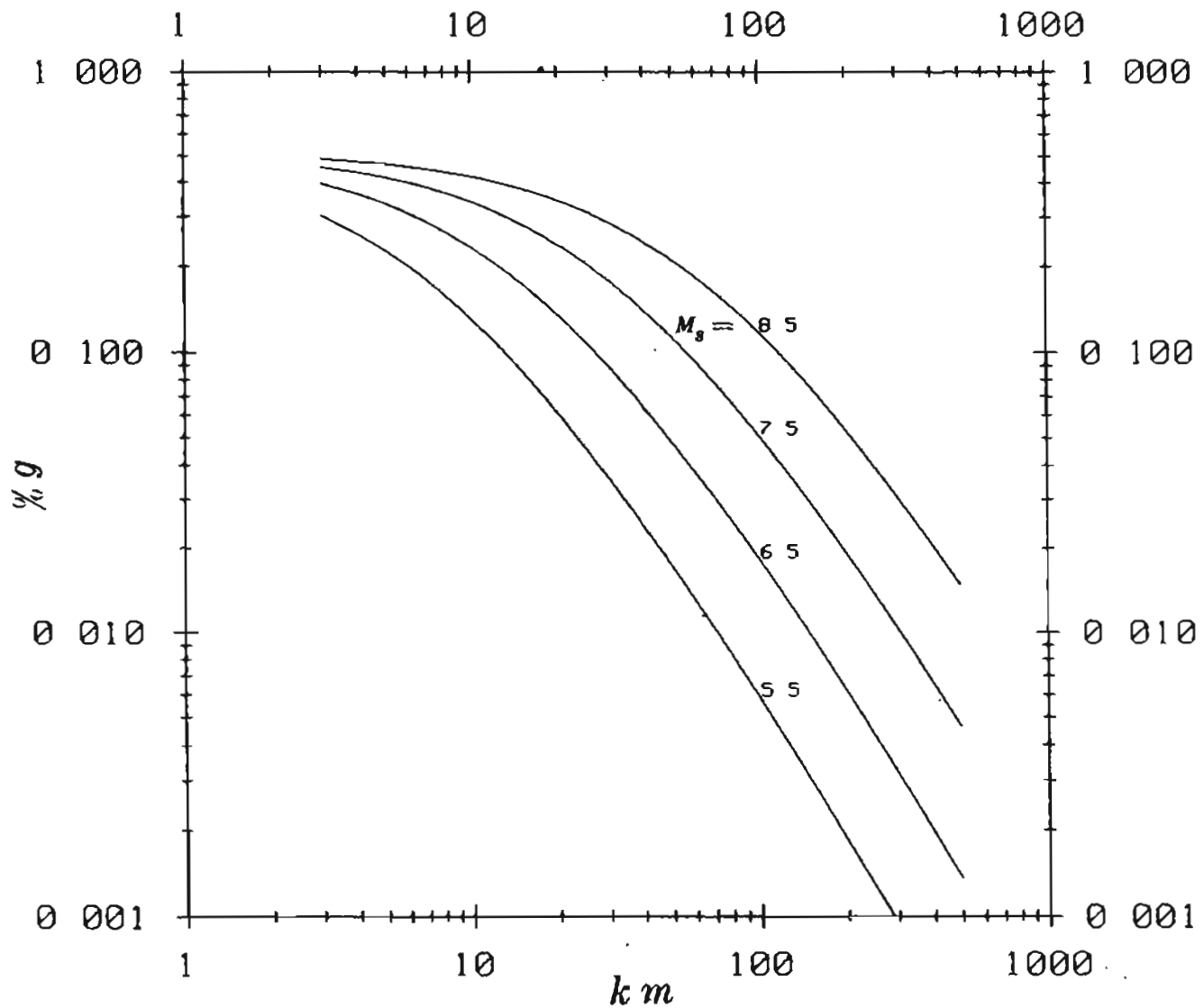

Figure 12. Campell (1981) attenuation relationships. Peak ground acceleration (in % of g) as a function of surface wave magnitude (M_s) and distance (in km).

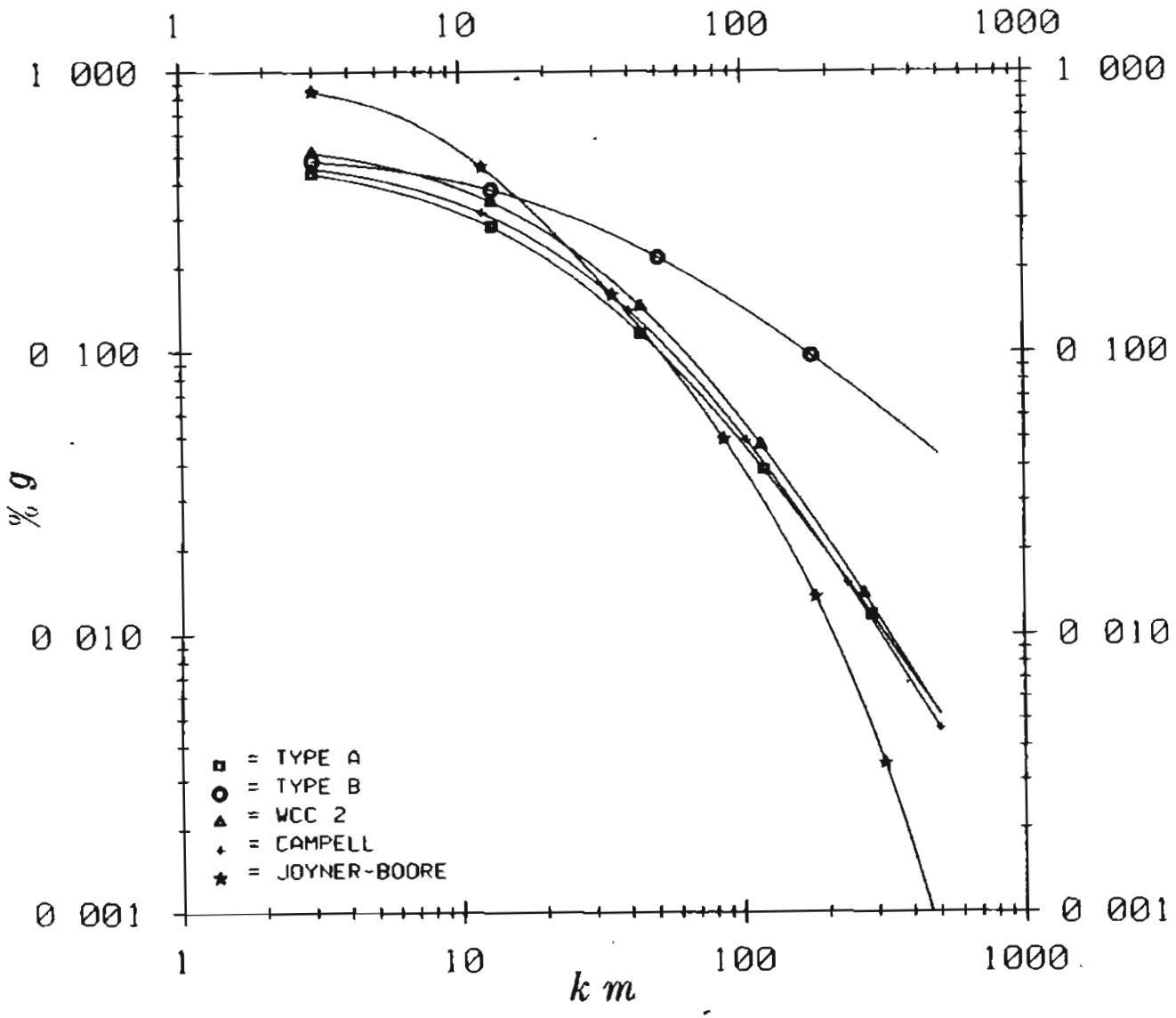

Figure 13. Comparison of attenuation relationships for M_s = 7.5 events. Peak ground acceleration (in % of g) as a function of surface wave magnitude (M_s) and distance (in km).

Table 4. Parameters of the attenuation functions for peak acceleration.

Parameter	OCS-A	OCS-B	WWC	Campell
B_1	191	284	80.14	15.9
B_2	0.823	0.587	1.1	0.868
B_4	1.56	1.05	1.75	1.09
C_1	0.864	0.864	0.315	0.0606
C_2	0.463	0.463	0.629	0.700
sigma	0.568[a]	0.700	0.400	0.372

$$\text{peak}(\text{cm/sec}^2) = \frac{B_1 e^{B_2 M}}{(R + B_3)^{B_4}} \quad \text{where } B_4 = C_1 e^{C_2 M}$$

[a]Standard error = 0.400 in this equation.

Attenuation is treated statistically, with an assumed log-normal distribution. Standard errors of regression analyses on which the attenuation relationships are based reflect the varying influence of particular source, path, and site effects with respect to which the data sets were not subdivided. For type-A relationships, a standard error of 0.568 is indicated, but a lower value (0.400) was used because two conditions that systematically seem to increase peak ground acceleration--reverse faulting mechanisms and steep local topographic relief--did not apply. The source zones for which the type-A relationship were used are characterized by strike-slip faulting; the topography of the NAG area is gentle. Both type-A and type-B relationships were derived from data recorded on stiff soils. The mostly unfrozen alluvial sands, water-saturated below 90 ft (R.A. Combellick, pers. commun.) seem better characterized as soft soils. In the absence of relationships derived for soft soils, application of stiff-soil relationships gives conservative results, because peak accelerations in soft soils are frequently lower than in stiff-soil or rock sites.

RESULTS AND DISCUSSION

The input parameters used resulted in an exposure value of 0.27 g for a 50-yr period and a 90-percent probability of nonexceedence. To this value, the northern random-source zone contributed 54 percent, the northern Benioff zone 24 percent, the eastern thrust zone 10 percent, and the Minto fault 10 percent. The remaining source zones contributed a total of 6 percent.

If the median curves of an attenuation relationship are used, exposure decreases 30 percent, to 0.19 g. If the original value of 0.568 is used for the standard error of the type-A relationships, exposure value increases to 0.31 g, a factor of 1.6 with respect to exposure values derived from the median curves. Using the WWC2 and Campell relationships for all sources, obtains values of 0.27 g and 0.22 g, respectively. Although WWC2 relationships are more conservative than type-A relationships, the same exposure values result, because, in the appropriate distance range, they are balanced by the yet more conservative type-B relationships used for the Benioff zone and shallow thrust zone. When the WWC2 curves are used, 100 percent of the exposure value is derived from the northern random zone. If type-A relationships are applied to all sources, a value of 0.23 g, comparable to that from the Campell (1981) relationships, is obtained. The Campell relationships are slightly more conservative, but this effect is offset by their slightly lower dispersion value.

Exposure is sensitive to the depth of the northern random zone. Raising and lowering it by 5 km from the depth of 15 km assumed here resulted in values of 0.29 g and 0.25 g, respectively. This is to be expected, because the rupture planes of earthquakes are horizontally oriented on the zone, and the depth of this source therefore controls the closest distance to the site. Data from local seismic networks with good control for hypocentral depth (Woodward-Clyde, 1982b; Estabrook, 1985) indicate a seismogenic zone about 20 km deep. There is no evidence for any interior Alaskan earthquake to have ruptured to the surface, so very shallow epicenters would be unlikely. Hypocenters of 10-km depth seem quite possible, but because strain release seems to occur preferentially along vertical faults, our modeling is conservative. Also, peak acceleration within a few kilometers of the fault will be--aside from site-specific considerations--influenced primarily by details of the rupture process. The controlling distance will be the distance to the closest patch of high-energy release on the inhomogeneous fault plane.

Because the northern random zone contributes the largest percentage to exposure value, changes in its seismicity rates have the greatest influence of any such changes. Doubling or halving the rates for this zone results in values of 0.30 g and 0.25 g, respectively. Because rates assumed for these zones are fairly conservative to begin with, doubling them seems unreasonable (implying 5.7 events of $M_S \geq 7$ in 80 yr within the zone). Equivalent changes for other source zones cause less than a 5-percent change in exposure value.

CONCLUSIONS

The exposure value for peak ground acceleration in the NAG area lies between 0.22 g and 0.29 g for a 50-yr period, with a 90-percent probability of not being exceeded. The value based on our best information for analysis input parameters is 0.27 g. This value is quite sensitive to choice of attenuation relationships, particularly whether or how the relationships are used statistically, and it is also sensitive to seismicity rates and depths of random source zones used to represent the intraplate seismicity of interior Alaska. The range of values indicated above reflects the range of reasonable assumptions one can make.

REFERENCES CITED

Abe, K., and Noguchi, S., 1983, Revision of magnitudes of large shallow earthquakes, 1897-1912: Physics of the Earth and planetary interiors, v. 33, p. 1-11.

Adkins, J.N., 1940, The Alaska earthquake of July 22, 1937: Bulletin of the Seismological Society of America, v. 30, p. 353-376.

Agnew, J.D., 1980, Seismicity of the central Alaska Range, Alaska 1904-1978: University of Alaska-Fairbanks unpublished M.S. thesis, 96 p.

Barnes, D.F., 1961, Gravity low at Minto Flats, Alaska: U.S. Geological Survey Professional Paper 424-D, p. D254-257.

Bickel, R.S., and Patton, W.W., 1957, Preliminary geologic map of the Nulato and Karteel Rivers area, Alaska: U.S. Geological Survey Miscellaneous Geologic Investigations Map I-249.

Brogan, G.E., Cluff, L.S., Korringa, M., and Slemmons, D.B., 1975, Active faults of Alaska: Tectonophysics, v. 29, p. 73-85.

Campell, K.S., 1981, Near-source attenuation of peak horizontal acceleration: Bulletin of the Seismological Society of America, v. 71, no. 6, p. 2039-2070.

Davies, J.N., 1975, Seismological investigations of seismotectonics in south-central Alaska: University of Alaska-Fairbanks unpublished Ph.D. thesis, 193 p.

_____, 1983, Seismicity of the interior of Alaska - a direct result of Pacific-North American plate convergence?: EOS, Transactions American Geophysics Survey, v. 64, p. 90.

Davies, J.N., Sykes, L., House, L., Jacob, K.H., 1981, Shumagin seismic gap: Journal of Geophysics Research, v. 86, p. 3821-3855.

Davis, T.N., 1960, A field report on the Alaska earthquakes of April 7, 1958: Bulletin of the Seismological Society of America, v. 50, p. 489-510.

_____, 1984, Alaska's earthquakes: Northern Engineer, v. 16, p. 8-13.

Davis, T.N., Estes, S.A., and Gedney, L.R., 1978, Probability of earthquake occurrences in the vicinity of the Chena flood control dam near Fairbanks, Alaska: University of Alaska Geophysical Institute Report UAGR-262, 32 p.

Dong, W., Shah, S.H., Bao, A., Mortgat, C.P., 1984, Utilization of geophysical information in Bayesian seismic hazard model: Soil Dynamics and Earth Engineering, v. 3, p. 104-111.

Estabrook, C.H., 1985, Seismotectonics of northern Alaska: University of Alaska-Fairbanks unpublished M.S. thesis, 138 p.

Hadley, D.M., and Helmberger, D.V., 1980, Simulation of strong ground motion: Bulletin of the Seismological Society of America, v. 70, p. 617-630.

Harding-Lawson Associates, 1984, Geological and geotechnical considerations, Knik Arm Crossing, Anchorage, Alaska: Anchorage, Report HLA Job 9620, 016.08, 131 p.

Hickman, R.G., and Craddock, Campbell, 1973, Lateral offsets along the Denali fault, central Alaskan Range, Alaska: Geological Society of America Abstracts with Programs, v. 5, p. 322.

Hickman, R.G., Craddock, Campbell, and Sherwood, K.W., 1976, The Denali fault system and tectonic development of southern Alaska: International Geologic Congress Abstracts, v. 3, p. 683.

Huang, P.Y., and Biswas, N.N., 1983, Rampart seismic zone of central Alaska: Bulletin of the Seismological Society of America, v. 73, p. 813-829.

Jacob, K.H., and Hauksson, E., 1983, Seismotectonic analysis of the seismic and volcanic hazards in the Pribilof Islands - eastern Aleutian Islands region of the Bering Sea: Contract NOAA-03-5-022-70 final report, 224 p.

Jacob, K.H., and Mori, J., 1984, Strong motions in Alaska-type subduction zone environments: World Conference Earthquake Engineers, 8th, Proceedings, v. 2, p. 311-317.

Joyner, W.B., and Boore, D.M., 1981, Peak horizontal acceleration and velocity from strong motion records including records from the 1979 Imperial Valley, California, earthquake: Bulletin of the Seismological Society of America, v. 71, p. 2011-2038.

Kienle, JÜrgen, Swanson, S.E., Pulpan, Hans, 1983, Magmatism and subduction in eastern Aleutian Arc, in Advances in earth and planetary sciences, arc volcanism, physics and tectonics: Tokyo, Terra Scientific, p. 181-224.

Molnar, P., and Taponnier, P., 1975, Cenozoic tectonics of Asia, effects of a continental collision: Science, v. 189, p. 419-426.

Mortgat, C.P., and Shah, H.S., 1979, A Bayesian model for seismic hazard mapping: Bulletin of the Seismological Society of America, v. 69, no. 4, p. 1237-1251.

Page, R.A., and Lahr, J., 1971, Measurements of fault slip on the Denali, Fairweather and Castle Mountain Faults, Alaska: Journal of Geophysical Research, v. 76, p. 8534-8563.

Patton, W.W., 1966, Regional geology of the Kateel River Quadrangle, Alaska: U.S. Geological Survey Miscellaneous Geological Investigations Map I-437.

Péwé, T.L., Wahrhaftig, Clyde, and Weber, F.R., 1966, Geologic map of the Fairbanks Quadrangle, Alaska: U.S. Geological Survey Miscellaneous Geological Investigations Map I-455.

Plafker, George, Hudson, Travis, and Richter, D.H., 1977, Preliminary observation on Late Cenozoic displacements along the Totschunda and Denali fault system: U.S. Geological Survey Circular C-751-A, p. B67-B69.

Ritsema, A.R., 1962, P and S amplitudes of the earthquakes of the simple force couple type 1: Bulletin of the Seismological Society of America, v. 52, p. 723-746.

St. Amand, P., 1948, The central Alaska earthquake swarm of October 1947: American Geophysical Union Transactions, v. 29, p. 613-623.

Schnabel, P., and Seed, H.B., 1973, Acceleration in rocks for earthquakes in the western United States: Bulletin of the Seismological Society of America, v. 63, p. 510-516.

Slemmons, D.B., 1977, State of the art for assessing earthquake hazards in the United States, report G: U.S. Army Corps of Engineers, Waterways Experiment Station, Miscellaneous Paper S-73-1.

Stout, J.H., Brady, J.B., Weber, F.R., and Page, R.A., 1973, Evidence for Quaternary movement on the McKinley strand of the Delta River area, Alaska: Geological Society of American Bulletin, v. 54, p. 939-947.

Thatcher, W., and Hanks, T.C., 1973, Source parameters of southern California earthquakes: Journal of Geophysics Research, v. 78, p. 8547-8562.

Thenhaus, P.C., Ziony, J.I., Diment, W.H., and Perkins, D., 1985, Probabilistic estimates of maximum seismic horizontal ground acceleration on rock in Alaska and the adjacent continental shelf: Earthquake Spectra, v. 1, no. 2, p. 285-306.

Tobin, D.G., and Sykes, L.R., 1966, Relationship of hypocenters of earthquakes to the geology of Alaska: Journal of Geophysics Research, v. 17, p. 1659-1667.

Weber, F.R., and Péwé, T.L., 1970, Surficial and engineering geology of the central part of the Yukon-Koyukuk lowland, Alaska: U.S. Geological Survey Miscellaneous Geologic Investigations Map 1-590.

Woodward-Clyde Consultants, 1982a, Development and initial application of software for seismic exposure evaluation, v. 2, Seismic exposure software calculation: San Francisco, Contract NA-80-RAC-000-91, final report, 122 p.

_____, 1982b, Final report on seismic studies for Susitna hydroelectric project: San Francisco, 155 p.

_____, 1982c, Anchorage office complex geotechnical investigation, Anchorage, Alaska, v. 1, Seismic hazards evaluation: San Francisco, 223 p.